

Chimera states in ensembles of fractally coupled oscillators

Lukas Rösel (315 225)

1st Corrector: Dr. Philipp Hövel

2nd Corrector: Dr. Astero Provata

January 8, 2016



Technische Universität Berlin

Abstract

In this thesis cantor sets were used to construct fractal networks of coupled kuramoto oscillators in order to search in them for chimera states. The cantor sets are able to produce complex coupling schemes that result in directed and undirected networks. In a number of these networks chimera states were found with unusual features like self-similarity and non-locality of synchronization. Insights about the unusual nature of networks were found like the necessity to view the ring-networks through other spatial representations in order to understand better the patterns of coherency and incoherency of the chimera states.

Abstract

In dieser Arbeit wurden Cantor-Mengen genutzt um fraktale Netzwerke aus gekoppelten Kuramoto Oszillatoren zu erzeugen und in diesen nach Chimära-Zuständen zu suchen. Die Cantor-Mengen produzieren komplexe Verbindungs-muster die in gerichteten und ungerichteten Netzwerken resultieren. In einer Anzahl dieser Netzwerke wurden Chimera-Zustände gefunden mit ungewöhnlichen Eigenschaften, wie Selbstähnlichkeit und Nicht-Lokalität der Synchronisation. Aus den Ergebnissen wurde die Notwendigkeit alternativer räumlicher Darstellungen der Netwerke ersichtlich, um die komplexen Muster aus Kohärenz und Inkohärenz weit entfernter Oszillatoren besser zu verstehen.

Hiermit erkläre ich, dass ich die vorliegende Arbeit selbstständig und eigenhändig sowie ohne unerlaubte fremde Hilfe und ausschließlich unter Verwendung der aufgeführten Quellen und Hilfsmittel angefertigt habe. Berlin, den

.....
Unterschrift

For my parents, Susanne and Jakob - *finally!*

Contents

1	Introduction	6
2	Theory	7
2.1	Kuramoto phase-oscillator	7
2.1.1	Local order parameter	8
2.2	Networks in mathematics	9
2.3	Cantor sets and fractals	12
3	Process	16
3.1	Constructing networks from cantor sets	16
3.2	Creating unique connected sets / choosing initial seeds	16
3.3	Calculations	19
4	Findings	20
4.1	[1 + 110011 ³] and [1 + 110011 ⁴]-networks	20
4.2	[1 + 11011 ⁴]-networks	22
4.3	[1 + 11000 ⁴]-networks	24
4.4	[1 + 1110110 ⁴] and [1101011 ⁴]	26
5	Conclusions	28
6	Possible further research	30
7	Appendix	32

1 Introduction

In 2002 Kuramoto and Battogtokh described a peculiar phenomenon [KUR02a]: they found the coexistence of coherent and incoherent parts in a network of identical non-locally coupled phase oscillators. It sparked huge interest and has been from thereon the subject of extended research. This hybrid state was named 'chimera state' by Steven Strogatz [ABR04]. The name is a tribute to ancient greek mythology, where the Chimera was a dangerous creature consisting of incoherent animal parts itself: It had two heads, one of a lion and one of a goat, and its tail was a snake. So like a chimera is a hybrid creature of different parts normally not expected to appear together, a chimera state is a hybrid state of synchrony and incoherence that was not expected to exist before 2002. Many researchers were intrigued by this new phenomenon and have since then joined in the research of this strange hybrid phenomenon.

The original discovery of Kuramoto was in a 1 dimensional ring-network with an exponentially decreasing coupling-strength depending on the distance of coupled nodes. Since then chimeras have been found in many different systems. They have also appeared in 2 or 3 dimensional networks. Different neurological oscillator models like the FitzHugh-Nagumo [OME13], SNIPER (Saddle Node Infinite Period) or Hindmarsh-Rose [HIZ13] model and a variety of others have been used and were able to produce chimera states. Recently chimeras have even touched down into mathematical knot-theory with the emergence of chimera-filaments that also form stable Hopf-Links, Trefoils and other knotted structures in 3-dimensional systems [MAI15, LAU2015]. In a recent publication many different aspects of chimeras have been compiled into a bigger overview of the material [ROD15].

Chimeras exists in the delicate balance of coherence and noise of coupled oscillatory systems. Because of that they have caught the eye of neuroscientists as well since this is also the realm in which the human brain operates. Dolphins and some species of birds are able to sleep with one side of the brain while the other stays awake. A possible explanation could be the partial coherence in one side and incoherence in the other side of the animal brain. Some neurological diseases like Parkinsons have been found to be correlated with an increased synchronization of certain regions of the brain [HAM07]. In other words, the brain of patients with Parkinsons-disease has left the healthy area middle of coherence and incoherence towards increased synchronization. Understanding chimera states could thus be important in for finding ways to cure such diseases.

Research in different ring-networks have been done to study aspects like stability, drifting, emergence or disintegration of chimera states in more detail [OME10a, OME11, OME12, OME13, OME15a]. In [OME15] the research was done in ring-Networks with a gap-coupled FitzHugh-Nagumo oscillators. Instead of coupling every oscillator within distance k some gaps were put in between. In this context the idea of increasing the number of gaps drastically by introducing a fractal coupling-scheme emerged. It resulted in some interesting high-order multichimera states.

Based on these results it seemed like a promising direction for further investigation of these networks.

2 Theory

2.1 Kuramoto phase-oscillator

A discrete version of Kuramoto's phase oscillator model is

$$\frac{d}{dt}\phi_i = \omega_i - \sigma^* \sum_{j=1}^N a_{ij} \sin(\phi_i - \phi_j + \alpha) \quad (1)$$

$$\sigma^* = \frac{\sigma}{\sum_{j=1}^N a_{ij}} \quad (2)$$

Here ϕ_i is a list of phases with index $i \in [1, N]$. ω_i is the inherent phase velocity of ϕ_i . The sum is describing the coupling to (mostly a subset of) other oscillators of a network. The strength of the coupling is mostly varied by a general parameter σ which is usually normalized by the number of coupled oscillators (beneath). The parameter α is the phase-lag parameter and it is used to fine-tune the attraction of coupled oscillators. For $-\pi/2 < \alpha < \pi/2$ coupled oscillators will tend to synchronize towards having the same phase with strongest attraction being at $\alpha = 0$. For values of $\pi/2 < \alpha < 3\pi/2$ coupled oscillators will act repulsive and will more likely stay within constant phase difference to each other (usually at $2\pi/N$ -th).

In the Kuramoto model each oscillator i is completely described by only 1 value; its phase ϕ_i . With each (discrete) timestep dt the phase is changing through its phase-velocity ω_i . If all parameters ω_i are the same the values can be set to $\omega = 0$ as if to view the system dynamics from a moving frame of reference. So each oscillator-state can be seen as a value moving around a circle meaning it can have values within the interval $[0, 2\pi]$ (see 1a). With $\omega = 0$ only the relative phase difference of coupled oscillators is changing the phase of the oscillators.

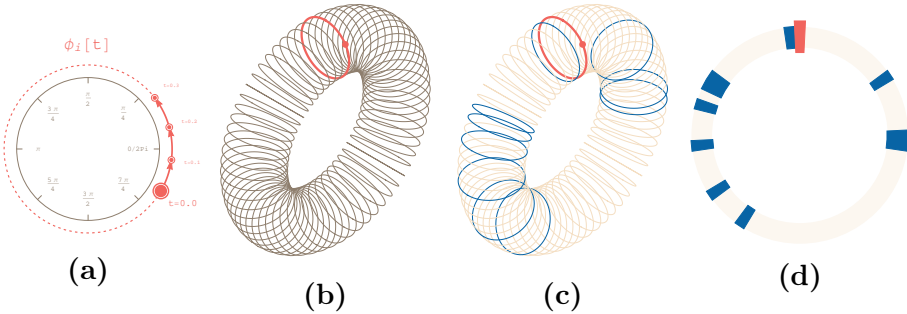


Figure 1 the state ϕ_i of an oscillator visualized as a point moving on a circle 1a. In a network there are multiple identical Oscillators that can be imagined as a torus 1b. In our model the angular velocity $\frac{dt}{d\phi}(t)_i$ of an oscillator i is influenced by a certain set of it's relative neighbors on the ring (here: only the state of the blue oscillators in 1c). The specialized pattern of connection can be visualized as in 1d. This visualization is used often in this thesis. The red element is at the topmost position and indicates an edge i which can be anywhere on the ring. The blue elements are all relative edges $i+k \rightarrow i$. Since the relative coupling distances (the values of $k = [k_1, k_2, \dots]$) are the same for every node) the image is describing the coupling scheme in full.

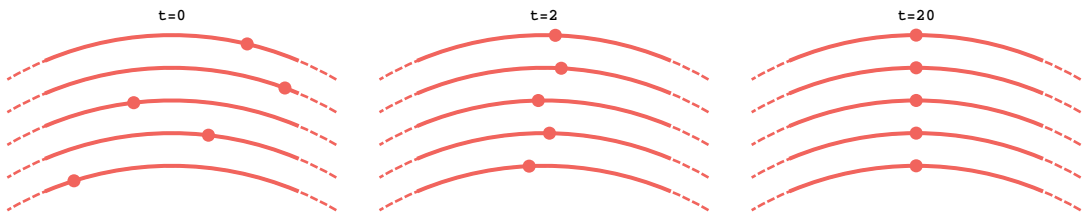


Figure 2 A small coupled distribution of (here 5) oscillators will after a while synchronize with the same phase if the right values are chosen like $-\pi/2 < \alpha < \pi/2$

2.1.1 Local order parameter

The local order parameter is a measure introduced by Kuramoto et al. in order to measure the coherence of phase oscillators in a local neighborhood of oscillators. It takes a set of phase values ϕ_i and puts out a measure for the coherency of the set. If the set is in perfect coherence (all values of ϕ are the same) the local order parameter will reach its maximum at $r = 1$. The formula

$$r_i = \left| \frac{1}{2k+1} \sum_{j=i-k}^{i+k} e^{i\phi_j} \right|$$

Is giving a measure for coherence of all oscillators within a distance of k to an oscillator i . The complex exponent of a value $\phi_i \in \mathbb{R}$ is a complex number on the unit circle in \mathbb{C} . Although all of the complex numbers have equal length, the absolute of the sum will only reach its maximum if the complex numbers are pointing in the same direction. The sum is also normalized by dividing of the number of oscillators in the distribution in order for the maximum to always be equal to 1. The idea is illustrated for a distribution of 25 phase values in 3.

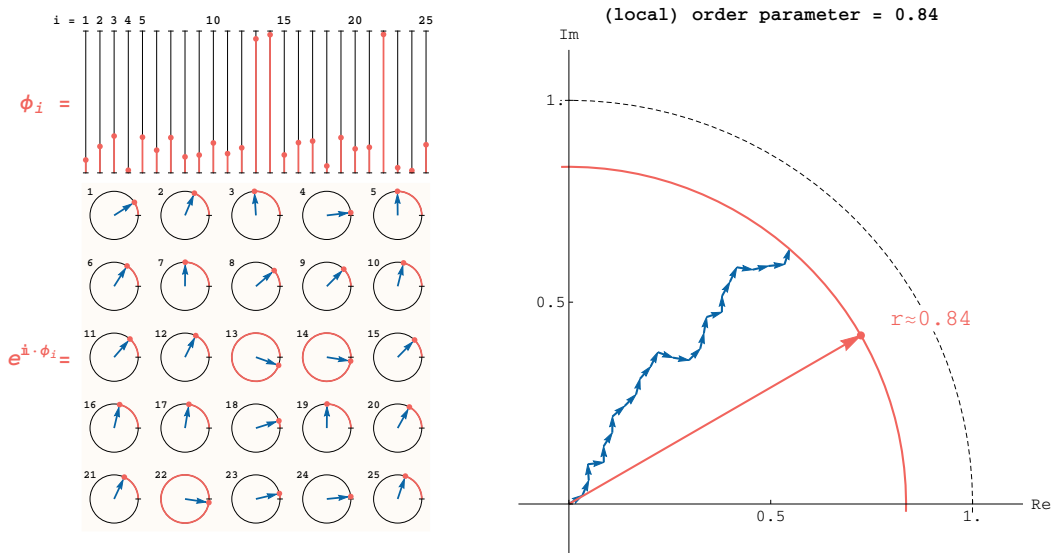


Figure 3 A distribution 25 of phase values (left, top) with its complex exponential values underneath. On the right side all arrows (divided by 25) are summed together and the absolute value is indicated as the radius of a red circle. In this example the values are already slightly synchronized and their arrows are going generally in the same direction, resulting in a high value of the order parameter: $r = 0.84$.

2.2 Networks in mathematics

In common words a network is a number of objects and connections between each other. In mathematics, a network (or 'graph') is described as 'vertices' or 'nodes' that are connected by 'edges'. The vertices are just identified by an index e.g. $i \in [1, 2, 3, \dots, N]$. Two vertices can be connected in different ways (see 4). There's a distinction made between directed and undirected Networks. In an undirected Network the edge $i \rightarrow j$ is equivalent to the edge of $j \rightarrow i$ whereas in a directed one it can be an important feature. Like the flow of information on the internet is going to and fro, but from a radio station it only goes in one direction. In principal any node can also be coupled with itself through the edge $i \rightarrow i$. As a network can be described by its edges which can be written as a double-indexed object, it seems natural to think of it as a matrix. This matrix is commonly referred to as the adjacency-matrix A of a network. A network with n vertices is thereby represented by an $n \times n$ matrix. If there exists an edge from vertex i to vertex j the element a_{ij} is equal to 1. For every missing edge a_{ij} is 0. The adjacency-matrix from an undirected network is identical to its transposed matrix $A = A^T$. Transposing the matrix of a directed Network means to reverse all the edges; $i \rightarrow j$ becomes $j \rightarrow i$ (see 5).

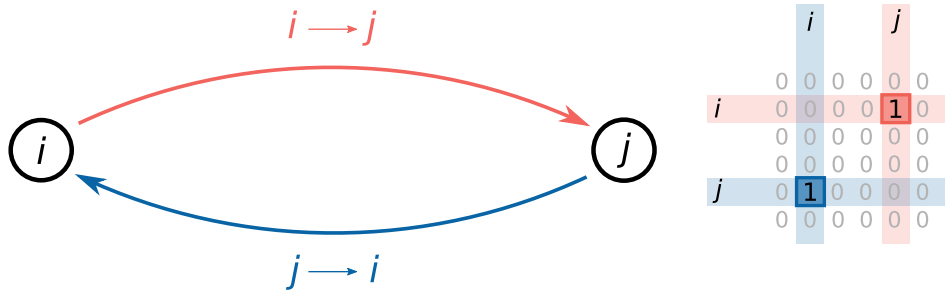


Figure 4 Two vertices i und j can be connected in 2 ways by the two edges $i \rightarrow j$ (red) and $j \rightarrow i$ (blue). In a network any edge has a start and an end. When represented as an adjacency-matrix A (right) the start is indicated by the row index and the end is indicated by the column index.

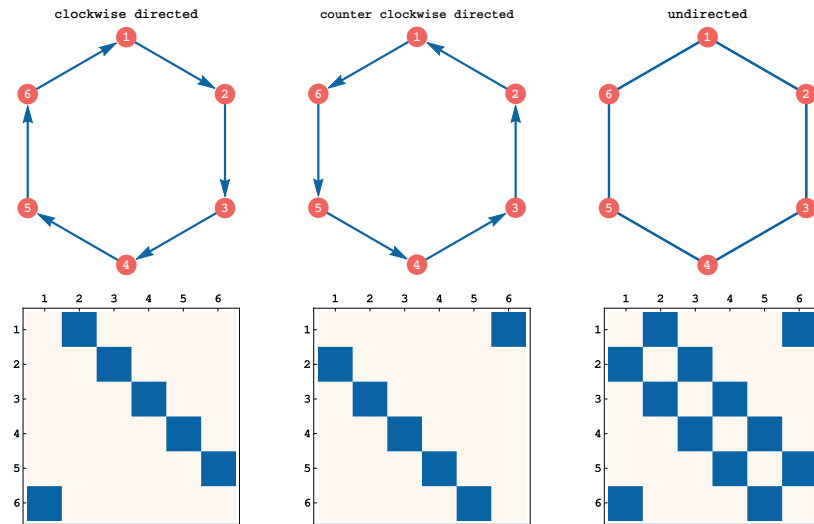


Figure 5 3 very simple ring networks of $N = 6$ vertices with directed and undirected (right) coupling and their corresponding 6×6 adjacency matrices underneath.

The representation of a network as a matrix is more abstract since it is free of any information about the spatial distribution of its nodes. But in order to understand the structure of networks it is often more natural to think of them as vertices embedded in 2 or 3 dimensions. For example we can take the skeleton of a Platonic Solid like the Dodecahedron. We may know a Dodecahedron as an object embedded in 3 dimensional space. Maybe we have used one as a 12-faced dice already. It has 20 vertices, 30 edges and 12 regular pentagons as faces. But if we see it as simply a network only the vertices and edges are left without any additional information about length of edges or position of vertices; we are free to choose other representations. Now we can either remain in 3-dimensional space where we can easily understand its symmetry or go into 2 dimensions (see 6).

In this particular example the 2d representation has the advantage of being similar to the form of the paper of this thesis - flat. The 3-dimensional view is in fact only a projection onto paper and results in some edges that are crossing over one another. This can be distracting so the flat representation is simpler. But in

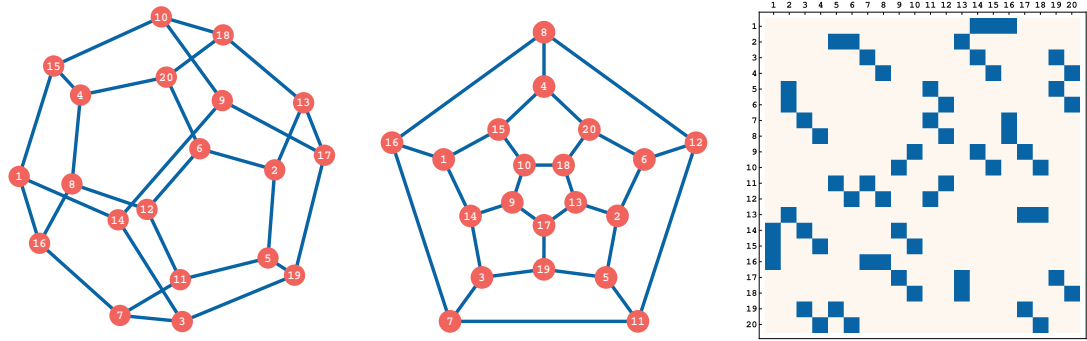


Figure 6 the undirected skeleton graph of a dodecahedron in 3-dimensional spatial representation (left), flat without crossing edges (middle) and as an 20×20 adjacency matrix (right)

more complicated networks even our 3 dimensions aren't enough to show some of the deeper symmetries that can exist in a network¹. It is therefore a good idea to not rely too much on a spatial representation but use other tools like adjacency matrices.

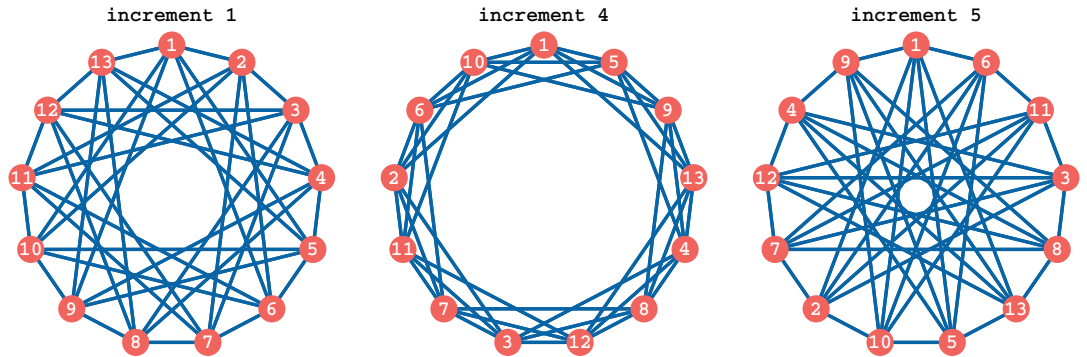


Figure 7 A ring network consisting of $N = 13$ vertices and edges $i \rightarrow i \pm k \bmod N$ with $k \in \{1, 4, 5\}$ (notice the gaps in the values for k) can have several equivalent representations. Here they are sorted by using 3 different increments to change the index along the ring. The middle sorting seems to be even better suited for understanding the coupling since it brings coupled vertices closer together than the natural one (with increments of 1).

A ring-graph is in its exact definition a set of N vertices where each is only connected to its immediate neighbors. In a directed graph a node i is connected to either $i + 1 \bmod N$ or $i - 1 \bmod N$, in an undirected one it is connected to both. But in the context of this work, we shall refer to all networks where the coupling of relative neighbors is invariant under rotation as ring-networks.

In some cases the spatial representation of a complex network can be even distracting. Since a ring-graph normally has local coupling (only local neighbors are

¹there exist for example 'polychora' which are the equivalent of platonic solids - only in 4 dimensions (like the 120-cell which is an object with 120 dodecahedrons as its boundaries). Since we are not able to see these objects in their natural habitat (4 dimensional space), we are not able to intuitively see the symmetries when looking at them in 3 dimensional representations.

connected) it is natural to sort them according to their index and position them on a circle. But with additional connections as it is with the k -nearest-neighbor-coupling the coupling becomes non-local. It is still intuitive to visualize it as a ring, because in most cases 2 coupled vertices are still near according to their indices. But with increasing number of non-local connections and also gaps within the quality of some visualization may be questioned. For example in 7 there are shown 3 different ways to visualize the coupling of the same network. The natural ordering (left) seems not to be the optimal sorting in order to show the coupling by bringing coupled nodes close together. This example is a simple one. The number of nodes is a Prime so all increments will result in ring-visualizations of all nodes. But for more complex coupled networks there may not exist a solution as simple as sorting by a different index. Some complex coupling schemes might result in different neighborhoods of vertices where most edges are connecting vertices within a neighborhood and only few connect the different neighborhoods. In such a case a visualization as a ring will not help but in some cases trivialize it and prevent a better understanding.

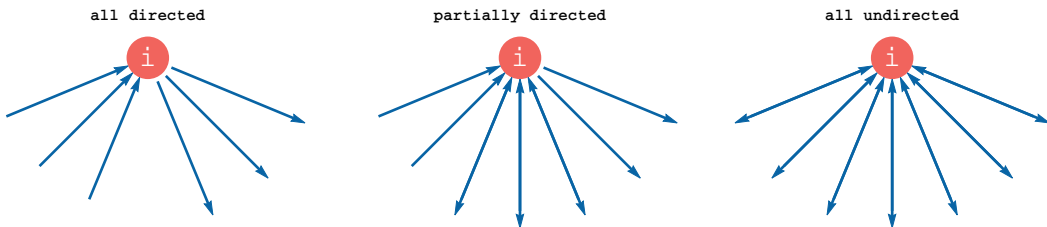


Figure 8 Due to the rotational symmetry of the ring network the number of incoming connections is always equal to the number of outgoing connections for all vertices i . Depending on the network the edges can be all directed, partially directed or completely undirected for symmetric adjacency matrices. That means if the coupling is reversed no changes in the number of incoming and outgoing connections occur. Therefore it is enough to only study one network out of any reversible pair.

2.3 Cantor sets and fractals

The Cantor-set in its classical representation is a set of points in \mathbb{R} that exhibits fractal properties. It was named after german mathematician Georg Cantor (1845 - 1918). There are 2 different approaches to the cantor set: top-down and bottom-up (further down) construction. The most common one is 'top-down': start with an interval like $[a, b]$ and remove parts of it. In this approach the set is produced by using a process $g : \boxed{\quad} \rightarrow \boxed{\quad} - \boxed{\quad}$. This process g is then used iteratively (see 9 for iterations $n = 0 - 7$) by re-using the result as input. In words g would be 'take an interval or a set of intervals and split each interval into 3 parts of equal length, then remove the middle part from the set'. The set of points after $n \rightarrow \infty$ iterations is the Cantor-set.

In 2-dimensions there's a similar fractal to the Cantor set called the Sierpinski-Carpet. A function f is defined by $f : \blacksquare \rightarrow \blacksquare - \square$. f can be used with different inputs e.g. $f : \blacksquare \rightarrow \blacksquare - \square$. Thus it can also be used iteratively by using its output as



Figure 9 Cantor-set with $b = [101]$ at iterations $n = 0 - 7$

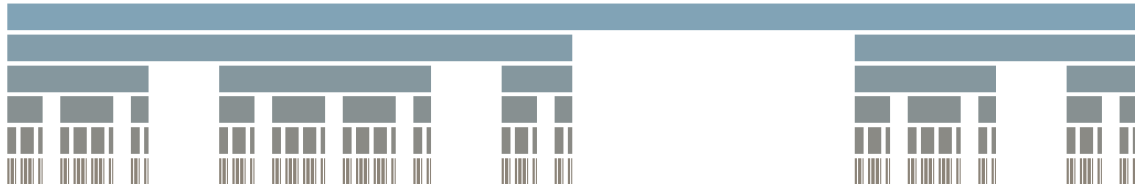


Figure 10 Cantor-set with $b = [1101]$ at iterations $n = 0 - 5$

input. It is then iteratively used on its own to produce ever more holes. The result after $n \rightarrow \infty$ iterations is called a Sierpinski-Carpet (see 11).

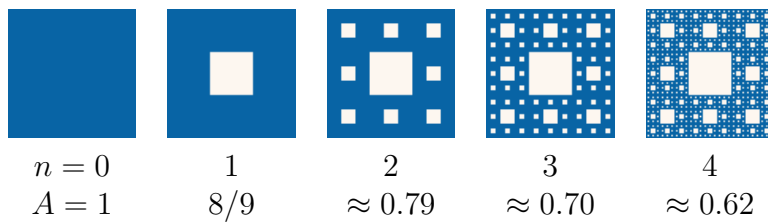


Figure 11 Several Iterations of the process which is used to gain the Sierpinski-Carpet. Underneath: the number of iterations and remaining area (blue).

With every use of g the number of points in the set corresponding sets is reduced to $2/3$ of its size. So the total number of points is decreasing with $(2/3)^n$. The cantor set is defined as all remaining points in the interval after $n \rightarrow \infty$ iterations which are paradoxically still infinitely many although $\lim_{x \rightarrow \infty} (2/3)^n = 0$. In the case of the Sierpinski-Carpet the area of the initial square $A_0 = 1$ with every use of f is reduced to $8/9$ th. So the area of the actual Sierpinski-Carpet is $\lim_{x \rightarrow \infty} (8/9)^n = 0$. Also the length of the boundary of A is increasing with every iteration and reaches ∞ for the Sierpinski-Carpet when $n \rightarrow \infty$. So the area is 0 while the boundary is ∞ .

This strange property relates to the fractal dimensions of fractals. The dimension of the Cantor-set d_{cantor} lies between 0 (a point) and 1 (a line). The dimension of the Sierpinski-Carpet lies between 1 and 2 (so it is something between a line and a surface). Typical objects have integer-type dimensions and we are used to derive the number by how many linear independent base vectors we need to describe them. E.g the dimension of a cube is $d = 3$ because we need 3 coordinates ($[x, y, z]$) to describe every position within it. A square has the dimension 2 because we only

object	line	square	cube
dimension	$\frac{\log 2}{\log 2} = 1$	$\frac{\log 4}{\log 2} = 2$	$\frac{\log 8}{\log 2} = 3$

Figure 12 the Hausedorff-dimensions of very simple objects.

need to 2 coordinates $([x, y])$ an a line has only 1 dimension.

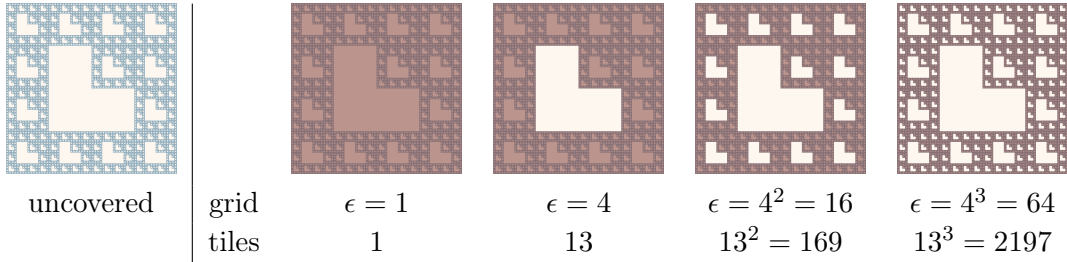


Figure 13 a fractal (left) can be covered by tiles positioned on a grid. By adding a number of subdivisions (ϵ) within the grid the fractal is covered more accurately

Another practical way to determine the dimension of an object is to completely overlap it with smaller objects of decreasing size (see 13). The way the number of needed (smaller) objects is growing can be used to calculate the dimension. For example a square \square_1 with edges $e = 1$ can be overlapped by the same square \square_1 one time. But there are $2^2 = 4$ smaller squares $\square_{1/2}$ needed to overlap \square_1 . Similarly there are $3^2 = 9$ squares $\square_{1/3}$ needed to overlap \square_1 . In general there are ϵ^2 squares $\square_{1/\epsilon}$ needed to cover \square_1 with $\epsilon \in \mathbb{N}$.

The dimension of an object then is

$$d = \frac{\log N}{\log \epsilon}$$

, where N is the number of elements scaled by $1/\epsilon$ needed to cover the object. With this method we can calculate the dimension of various things. It is called the 'Hausdorff-dimension' of an object.

In 15 there is another example where changing the representation or coordinate system can help to understand things. The fractal curve is meandering all over the paper and eventually will fill a certain area. After $n \rightarrow \infty$ iterations the line has essentially transcended into the 2nd dimension. But even before with finite iterations n it is becoming very complex very quickly. Understanding relations between points of the line may require changing the coordinates to a 2 dimensional system (like finding the shortest distance between 2 points). So in the same way as a line can become a surface through adding more and more layers of complexity, a ring network can possibly through increasingly complex non-local coupling outgrow its initial representation (In fact the network as its adjacency matrix should sometimes be the first step in understanding a network, before it is represented in a coordinate system).

An alternative way to think about the cantor set is the 'bottom-up' construction. It is also the one used in this particular application. Hereby we start with a list or

object	cantor set $b = [101]$	sierpinski carpet	example in 13
dimension	$\frac{\log 2}{\log 3} \approx 0.63$	$\frac{\log 8}{\log 3} \approx 1.89$	$\frac{\log 13}{\log 4} \approx 1.85$

Figure 14 the Hausdorff-dimension of several fractals.

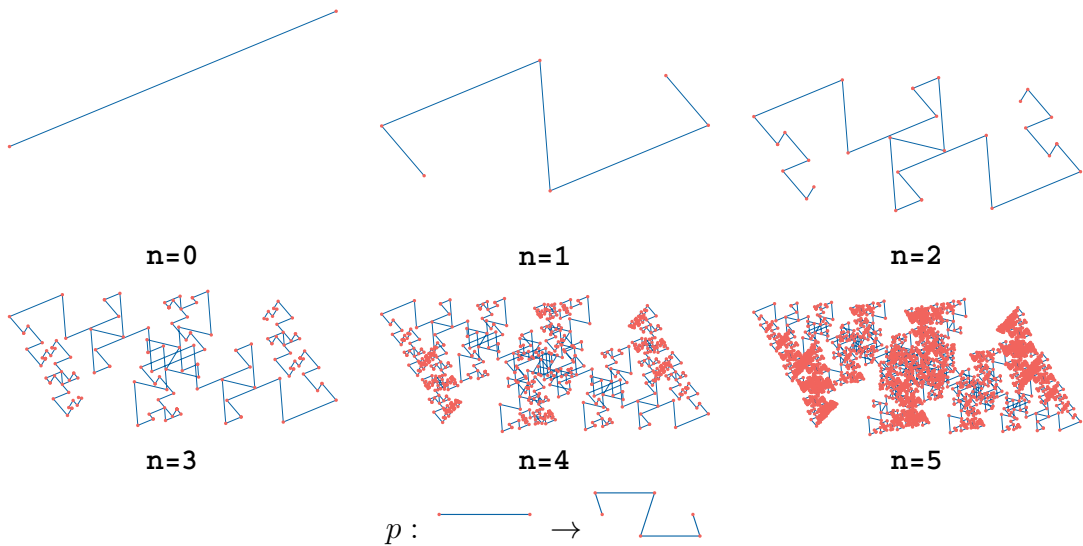


Figure 15 A fractal that is created by a simple process p where a line segment is replaced by a different set of line segments while leaving the start end end point there. Although the fractal is still a 1 dimensional line, after few iterations the structure becomes so complex that it seems easier to identify points by a different (2 dimensional) coordinate system. Some features of the fractal, like intersections of the line with itself might even be missed when staying in the 1 dimensional coordinate system only.

n	<i>cantorsset</i>	<i>length</i>
0	1	1
1	101	3
2	101000101	9
3	101000101000000000101000101	27

Figure 16 Bottom-Up construction of a cantor set with base $b = [101]$.

seed that we will call the 'base b '. It contains only binary numbers 0 and 1 (Later, a 1 will mean there's an edge and 0 will mean there's no edge).

the bottom-up construction is made by starting with a set of just one element and using a simple replacement rule iteratively. Every element c_i of a set $c = [c_1, c_2, c_3, \dots, c_l]$ is replaced by the rule

$$c_i = \begin{cases} b, & \text{if } c_i = 1 \\ b \times 0 & \text{otherwise} \end{cases}$$

for one iteration.

But only if the element $c_i = 1$. $b \times 0$ means an empty set of the same length as b . See 16 for the process starting at $c = [1]$. The length N of this cantor list is growing exponentially with $N = b^n$. So the sets become huge very fast. The cantor set c after n iterations shall be referred to as $c = [b^n]$. The set $b = [11011]$ after 3 iterations shall be $[11011^3]$. When another (single) element is added (appended) to the left side of the set *after* going through n iterations the set shall be referred to as $[1 + 11011^n]$.

3 Process

3.1 Constructing networks from cantor sets

How does a fractal network look like? In the context of this work a fractal network shall be a network with its adjacency matrix A derived from a cantor set c . The approach used here is to create a cantor set in the form of a vector with ones and zeros. The cantor set is then used to create a circulant adjacency matrix $A(c)$ by using the set for every row, but shifting it to the right one step further for every next row. The coupling term of a vertex or oscillator i to itself (any edge $i \rightarrow i$) is not depending on the state of the oscillator itself ($\phi_i - \phi_i = 0$) but only from the phase-lag parameter α . So in order to make the first element of the cantor set more useful in the resulting adjacency matrix we can choose to add a 0 to the left side of the cantor set (see 17 for transformation from set to matrix). By doing so we also create a symmetrical coupling scheme for any cantor set derived from a symmetrical base (e.g. $b = [11011]$). Without the added zero there would be a slight asymmetry since either the last left or last right element will be used for edge $i \rightarrow i$.

$$a_{ij} = v_{i^*[i,j]} \quad (3)$$

$$i^*[i,j] = (i + 1 - j \mod N) \quad (4)$$

We can use this formula (3) to turn a vector into a matrix; $v \in \mathbb{R}^N$ and $i, j \in [0, 1, 2, \dots, N]$.

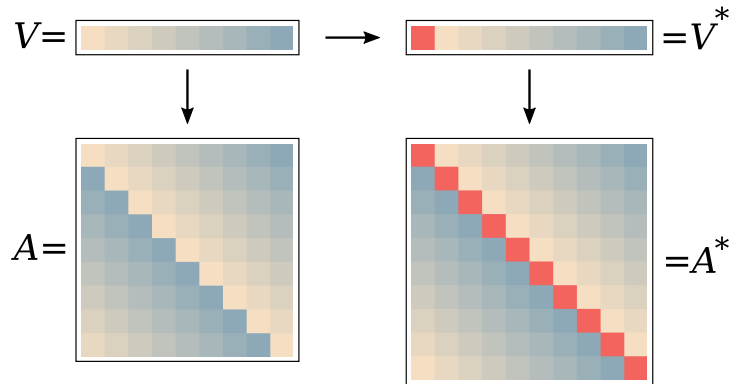


Figure 17 creating a circulant matrix from a vector as by (3). Right: By adding a new first element $\blacksquare = 0$ we can shift the former first element from edge $i \rightarrow i$ to edge $i \rightarrow i + 1$. In this thesis the method on the right has been used at all times.

3.2 Creating unique connected sets / choosing initial seeds

When choosing lists consisting of elements 1 (edge) and 0 (no edge) for the use as b , a lot of different possibilities present themselves. For any length l of the initial

base length	3	4	5	6	7	8	9	10
interesting bases	2	6	15	31	66	130	265	521

Figure 18 The number of possible bases to choose from with lengths $l \leq 10$.

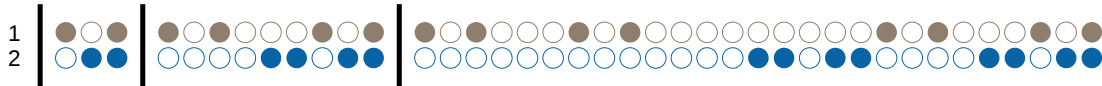


Figure 19 Both non-empty, non-full, non-single and reversibly-unique tuples tuples with length $l = 3$ consisting of 1 = ● and 0 = ○ on the left with their first (left), second (mid) and third (right) cantor iterations.

b there are 2^l possible l -tuples to choose from. But not all of these l -tuples are interesting to use for b , since we are searching for **fractally** connected networks we can remove some. From all tuples we remove

- empty sets: [000], [0000], [00...0]...
they will remain empty for every iteration and result in an empty graph (a 'non-network')
- full sets: [111], [1111], [11...1] ...
they remain full and create complete graphs (an 'all-to-all' network)
- sets with only one non-zero element: [100], [010], [001], [1000], [0100], ...
these result in either one or separate simple ring-graphs
- for every reversible pair like [110] and [011] we remove one.²

After sorting out all 'boring' sets there still remains a great number of them. with increasing base length the number increases dramatically. After all for *each* base can be iterated a different number of times in order to create networks of different sizes. In 18 the number of all useful tuples with length $l \leq 10$ is shown.

In rare cases after sorting out boring sets a base b can still result in a coupling scheme that creates several non-connected networks ³. This however was not the case in any of the few cases that were studied here.

³Similar to a network of $N = 10$ nodes with edges $i \rightarrow i + 2$ that results in two rings - one connecting all even numbered nodes, the other connecting all odd ones. To avoid this case at least one coupling distances $k \in [k_1, k_2, \dots]$ or one of the absolute differences of any $k_i - k_j \pmod{N}$ with $i, j \in [1, N]$ should not be a Divisor of multiple (\pmod{N}) of a Divisor of N (meaning the Divisors without 1 and N).

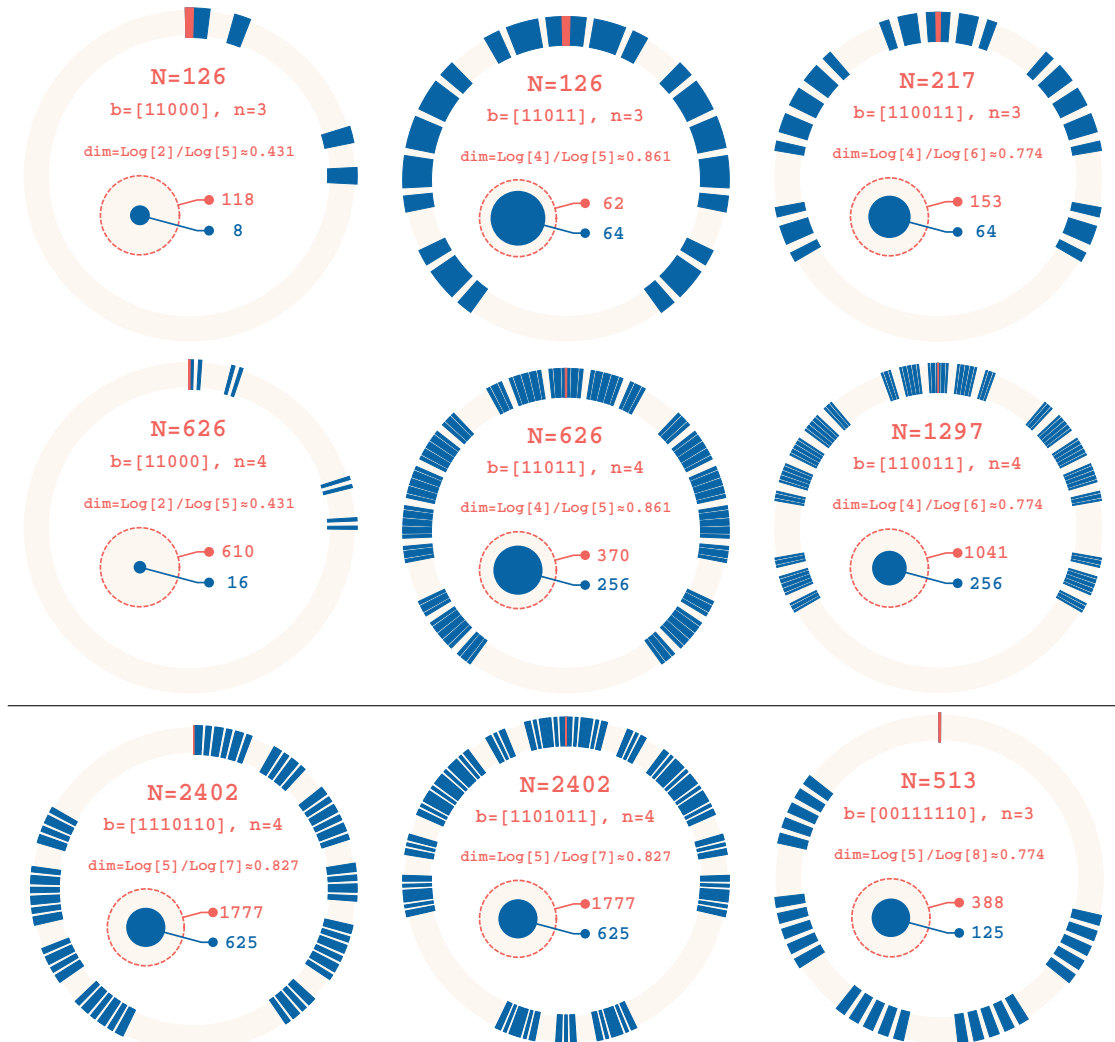


Figure 20 Visualizations for the coupling of a vertex i (red, 12-o'clock-position) to its relative vertices on the ring. visualized for different bases b with additional information (number of total oscillators in the network N , base b , dimension of the cantor set \dim and the number of coupled (blue) and uncoupled oscillators to one node).

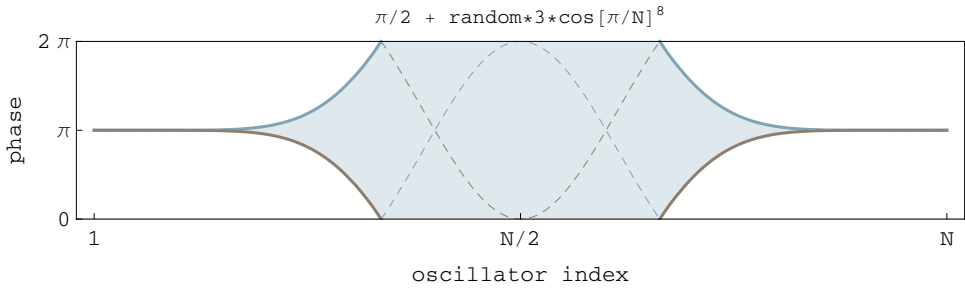


Figure 21 The initial conditions were random distributions shaped to be within the blue area.

3.3 Calculations

Once a base b was chosen an iteration number n was set and put in a python program. All calculations started with shaped random conditions (see 21). The initial distribution of phases $\pi_i[t_0]$ was generated by modulating a uniform random distribution:

$$\phi_i[t_0] = \pi + \text{random}[-\pi, \pi] \times \cos[\pi i/N]^8$$

Here $\text{random}[-\pi, \pi]$ denotes a uniform random distribution between $-\pi$ and π . The Cosine is taken to the power of 8 in order to move values near 0 closer together and create a coherent part in the initial distribution. The setup of the network structure was done by using the 'graph-tool' python package, differential equations were solved by using the 'Dopri5' integration method provided by the 'Numpy' python package. The absolute error tolerance parameter was set to $atol = 1e - 4$ (0.0001) and later decreased to $atol = 1e - 6$ (0.000001) after some testing showed very small deviations. In a couple of tests the impact of different error tolerances down to $atol = 1e - 20$ was tested. No further enhancement could be seen when decreasing it past 10^{-6} .

In the networks where calculations were made, the parameters $\sigma \in [0.05, 1.5]$ and $\alpha = 1.46$ were chosen. In some initial trials other values for α were tried, but never resulted in a chimera state. When a chimera state was found it was then used as input and the value of σ was changed in order to see if the pattern was only stable for the value of its emergence. In all cases the patterns showed to remain stable for values within the initial interval $[0.05, 1.5]$. So in most plots the coupling strength is $\sigma = 0.5$ since the plotted data came from a second calculation with the first calculations' results as initial conditions.

4 Findings

4.1 $[1 + 110011^3]$ and $[1 + 110011^4]$ -networks

In $[1 + 110011^3]$ - and $[1 + 110011^4]$ -networks single- and multi-chimeras emerged and remained stable for different values of σ within $[0.05, 1]$. The number of coherent regions was always a power of 6. Single, 6-fold and 36-fold multi-chimeras were found themselves. A 216-fold multi-chimera was produced by using a 36-fold chimera from a network with $n = 3$ cantor iterations and using this state as initial condition if a network with $n = 4$ iterations. This could be done by simply repeating it 6 times (the length of the base b). The 261-fold one didn't emerge itself. This could be due to the shaped initial conditions. It turns out that by sorting the oscillators not with increments of 1 but 6, $6^2 = 36$ and $6^3 = 216$ a single or multi-chimera state can be turned into each of the other ones (see 24).

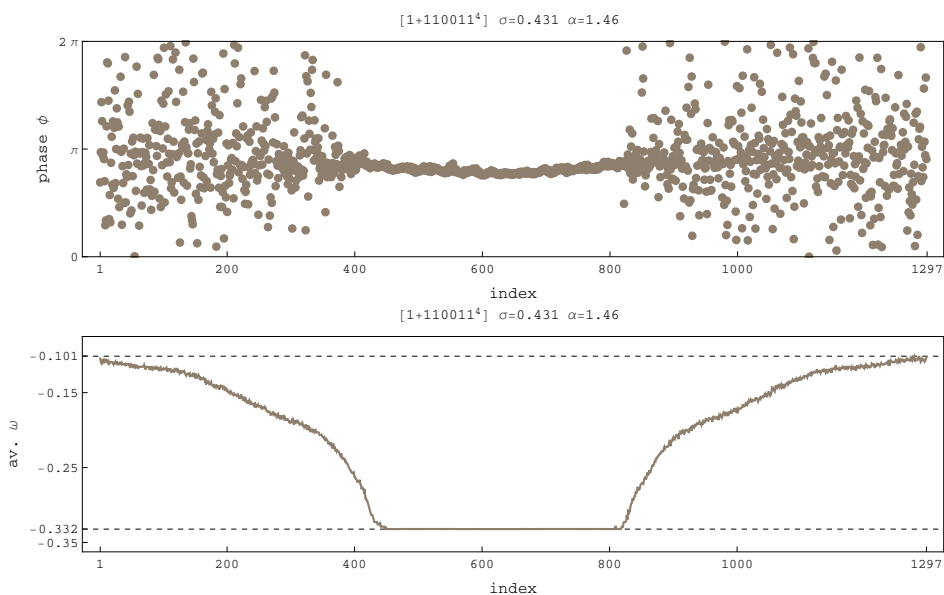


Figure 22 A single chimera state in a $[1 + 110011^4]$ network.

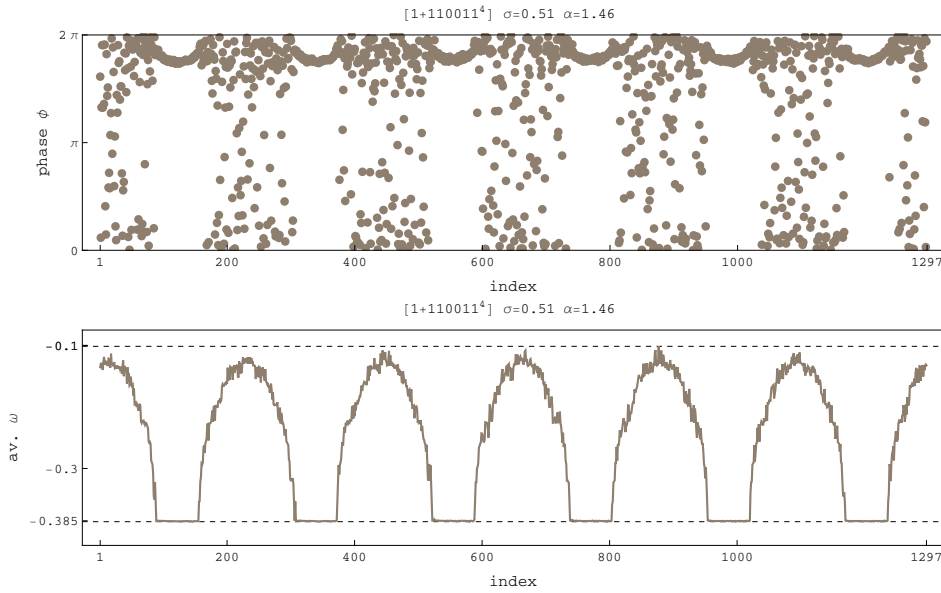


Figure 23 A 6-fold multi-chimera state in a $[1 + 110011^4]$ network.

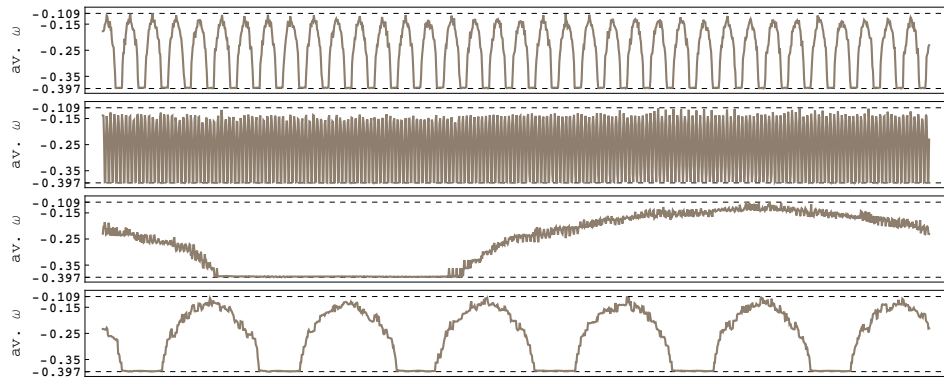


Figure 24 By changing the increment of the oscillators around the ring (see 7) all 4 chimera states that have previously been found in the network can be realized. The topmost graph is the natural order ($i = i$) of the $N = 1297$ oscillators, the other plots have the oscillators sorted with indices $i_6 = 6 * i \bmod 1297$, i_{36} and i_{216} (from up to down). The index has been omitted in the plots itself to avoid confusion.

4.2 $[1 + 11011^4]$ -networks

In $[1 + 11011^3]$ -networks the chimeras were not as expected 5-fold multichimeras but some kind of non-equally distributed triple chimera and a comb-like chimera (see ??). It turns out that both chimera states can be regarded as being the same but in a different representation of the network. As shown in 7 a network with rotation-invariant coupling can be sorted in a different way. When changing the increment of adjacent oscillators from 1 to 5 the comb chimera is turned into a chimera state that looks like the triple-chimera. Since in this network edges are $i \rightarrow i \pm k$ with $k \in [1, 2, 4, 5, \dots]$ it is easily justifiable to change the increment from 1 to 5. In both states the same coupling strength $\sigma = 0.5$ is used and leads to the same minimal and maximal values of the average velocity. The motivation for the separation of data-points in 5 groups is shown in 27.

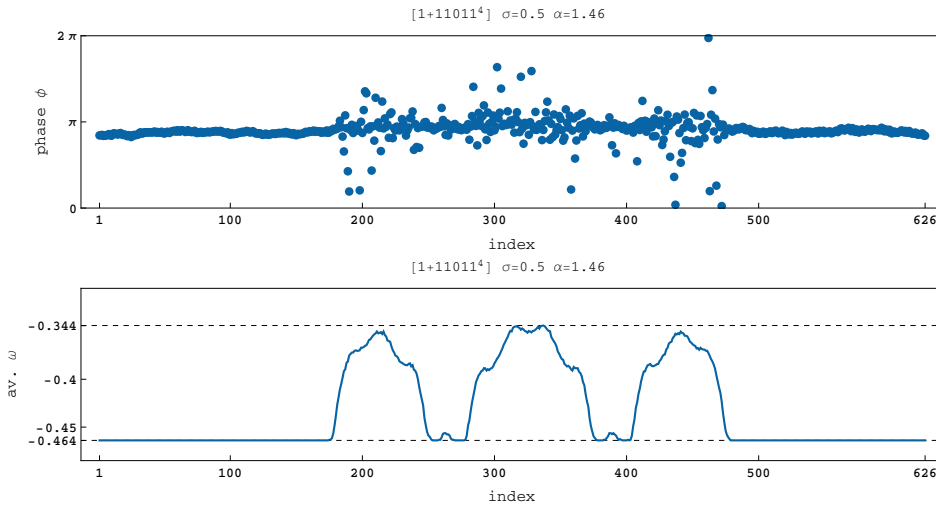


Figure 25 A triple chimera state in a $[1 + 11011^4]$ -network. The 2 smaller 'bulbs' are consistent.

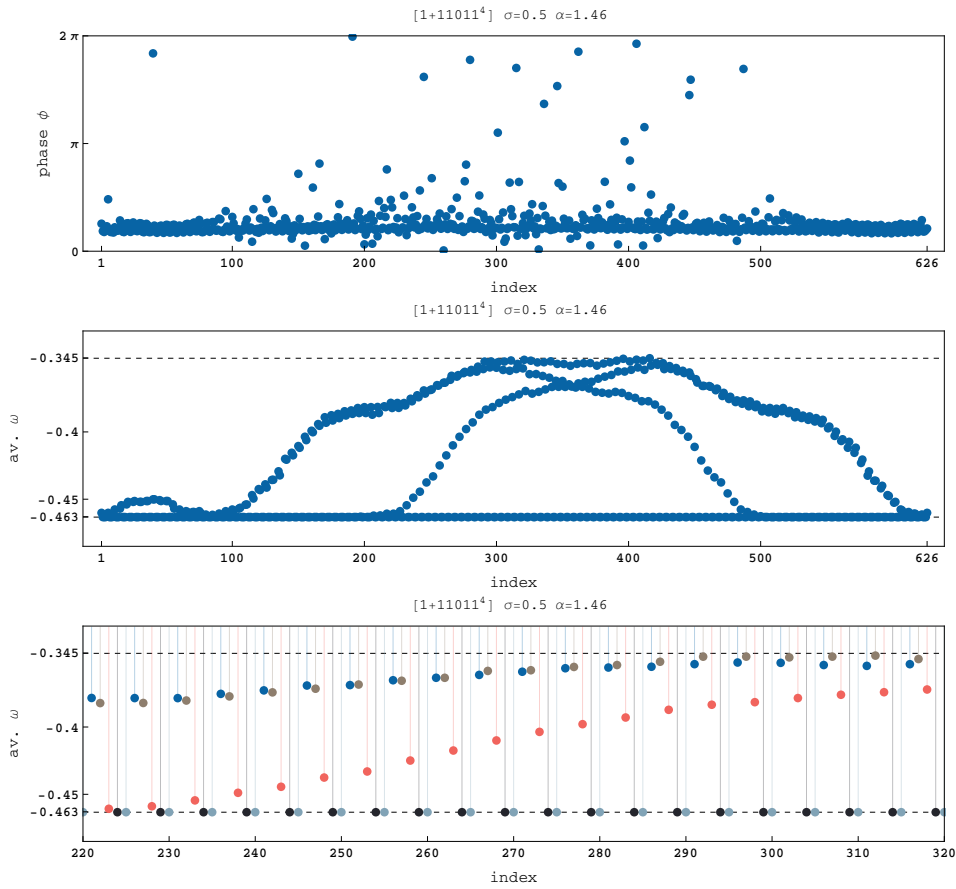


Figure 26 Phase and mean velocity profiles (top, mid) of the second chimera state found the network. When looking at the velocity profile more closely (bottom) it appears that values split into 5 groups. To make the grouping more apparent we can color the average velocities in 5 different colors: 1 | 2 | 3 | 4 | 5 | 6 | 7 | 8 | 9 ... etc.

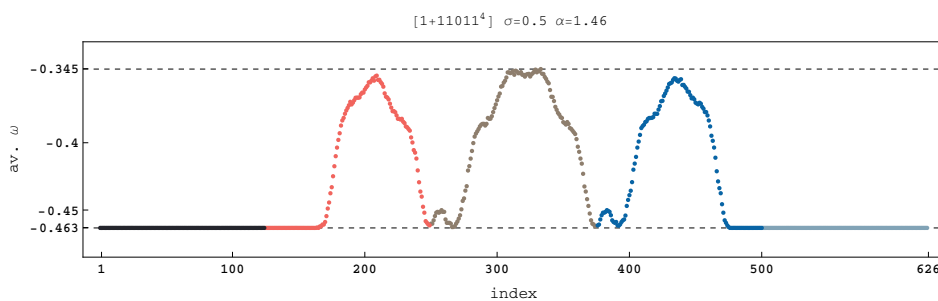


Figure 27 When stitching the 5 groups after each other (like shown above) in reverse order we get a chimera state that is very similar to if not exactly the one shown before in.

4.3 $[1 + 11000^4]$ -networks

In $[1 + 11000^4]$ -networks which consist of 626 oscillators 2 different chimera states were found. We shall call them A and B. Both were traveling chimeras due to the asymmetric coupling (oscillators are more influenced from the right than from the left therefor patterns travel from right to left). The patterns showed some self similarity which is a fractal property. This can be seen in the velocity profile in 28 where the incoherent regions with slowest (sometimes positive) velocities are 4 times (mid) repeated. In the magnified segment (bottom) one of the 4 slower moving parts is actually a pattern with 4 bulbs. If one looks closely even these bulbs are actually still subdivided into 4 bulbs. It is also possible to say that the bulbs are modulated with smaller bulbs. The local order parameter (with $k = 5$) is under both chimera states. The 4 repetitions in the pattern are indicated. For chimera B there is also a second pattern with 6 bulbs that is repeated 4 times. Both numbers 4 and 6 are one off of 5 which is the length of the original base. In other networks like $[1 + 1110000^3]$ this behavior can also be studied (see appendix for more examples).

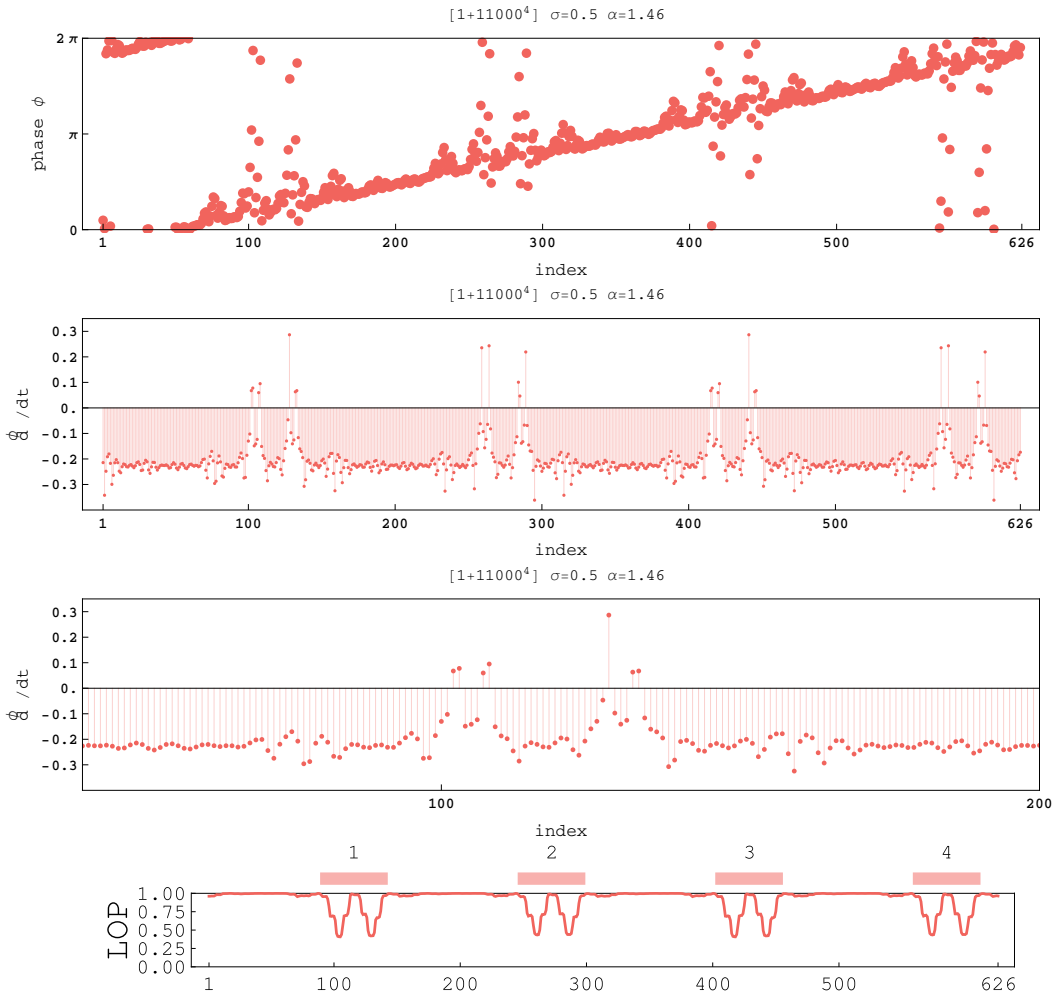


Figure 28 phase profile (top),velocity profile (mid, bottom) of chimera pattern A .

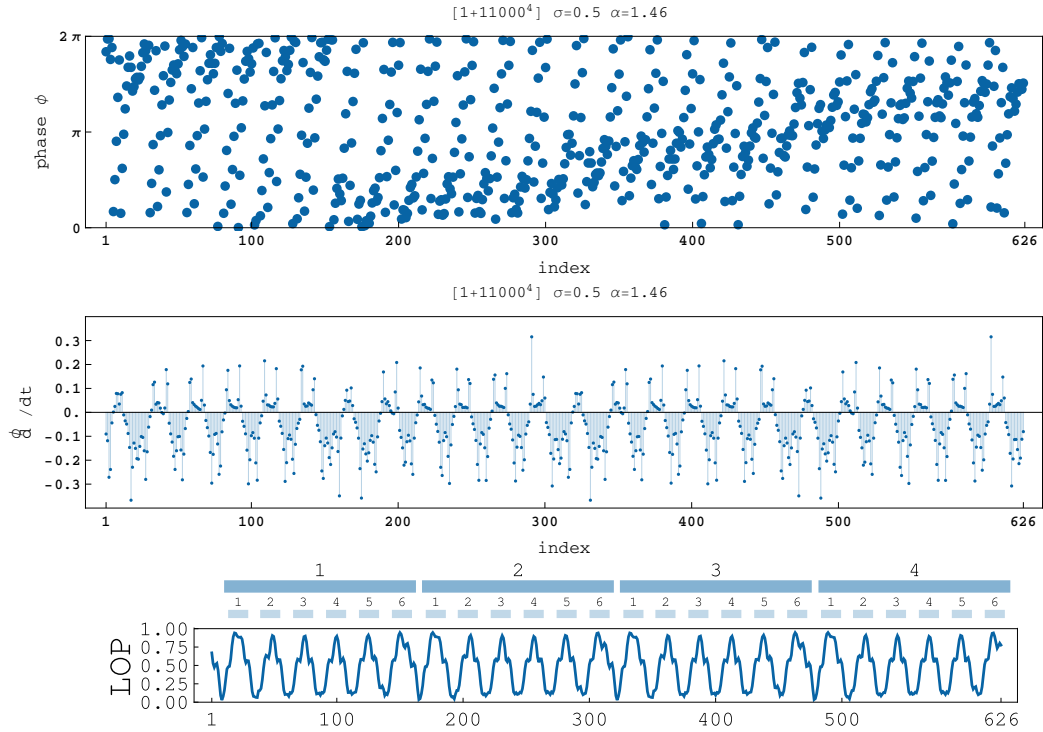


Figure 29 Chimera pattern **B** in a $[1 + 11000^4]$ -network with its phases and velocity profile. Since the Chimera is slowly traveling to the left, it will be shifted when plotted for different timesteps.

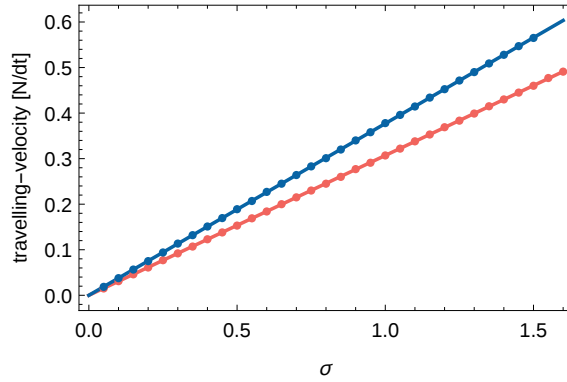


Figure 30 The travelling velocity of the two chimera configurations *A* and *B* depends differently on the coupling-strength σ .

Both types of chimera-patterns are travelling chimeras, because of the asymmetrical weight in the coupling scheme (oscillators are influenced more strongly by oscillators on the right). Both chimera-states *A* and *B* are depending differently on σ : Both increase when σ is increased, but in *B* the growth is higher ($v_{tr,A} = 0.377N/dt$, $v_{tr,B} = 0.307N/dt$) (see 30).

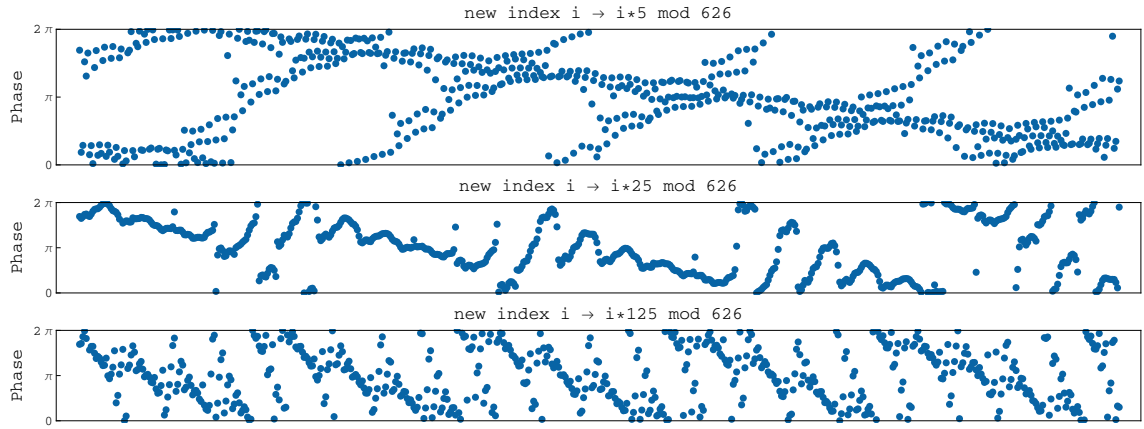


Figure 31 The chimera state B (of $[1 + 11000^4]$) with a different order of the oscillators. By sorting the oscillators not with their natural index i but with a new index $i_5 = i * 5 \bmod 626$ the different patterns can be viewed also. The index has been omitted from the plot to avoid confusion. Adjacent blue dots are 5, 25 or 125 steps apart. The sorting in the middle seems to show coherent parts much better than the sorting with increment 1 (see 29).

4.4 $[1 + 1110110^4]$ and $[1101011^4]$

For networks constructed with bases b of length $l = 7$ only two different examples are shown here. In one network a $12 * 7 = 84$ -fold multi-chimera structure was found. When investigating the average phase velocity profile there is a 12-fold arc structure and within each arc there is a fine 7-fold pattern (see). This is also a traveling chimera. The bigger 12-fold pattern is traveling to the right, whereas the fine substructure is staying in place (at least for the 2000 timesteps of the calculation).

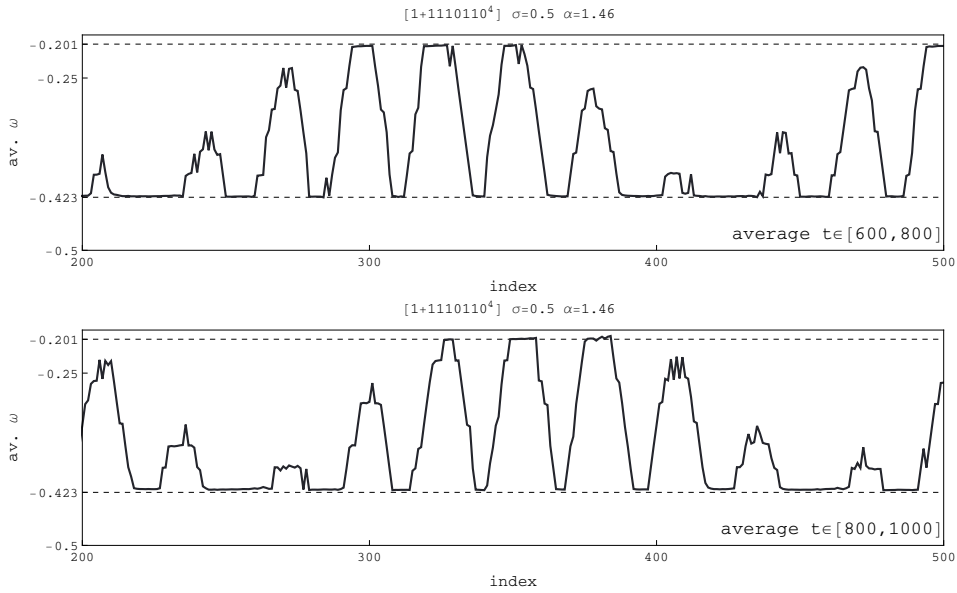


Figure 33 two magnified sections of averaged phase velocities. Intervals were $t \in [600, 800]$ (top) and $t \in [800, 1000]$ (bottom). The envelope structure has moved to the right for the later average whereas the fine structure remains in place.

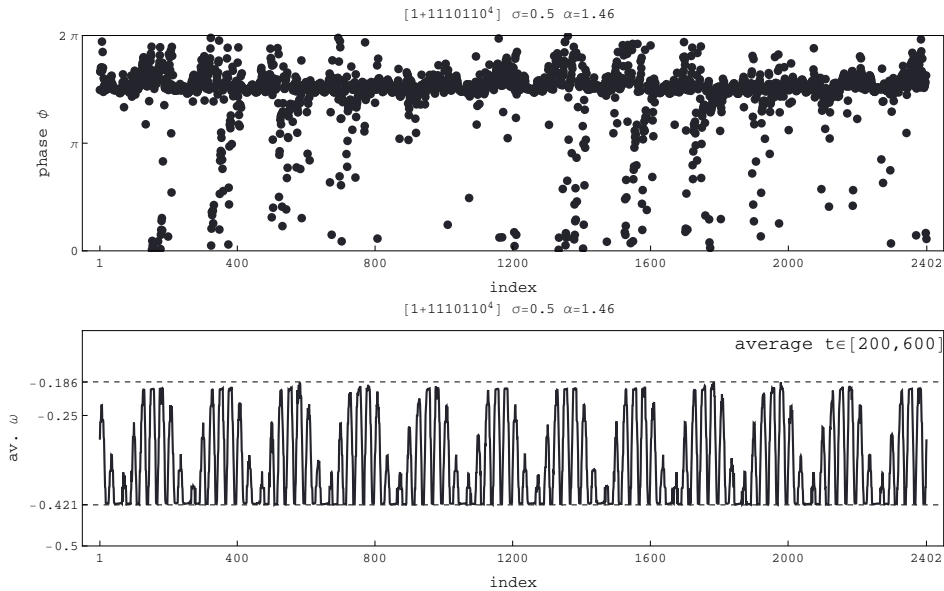


Figure 32 a 12-fold chimera with a 7-fold substructure. The phase velocities have been averaged only for a small interval because although the fine substructure is seemingly standing still, the global 12-fold envelope is traveling to the right.

Another interesting example was the $[1101011^4]$ -network. Here a 5-fold multi-chimera was found. Besides having 5 incoherent regions the pattern is similar to the chimera found in the $[1 + 11011^4]$ -network. Both chimeras have coherent regions of non-equal length between the incoherent oscillators.

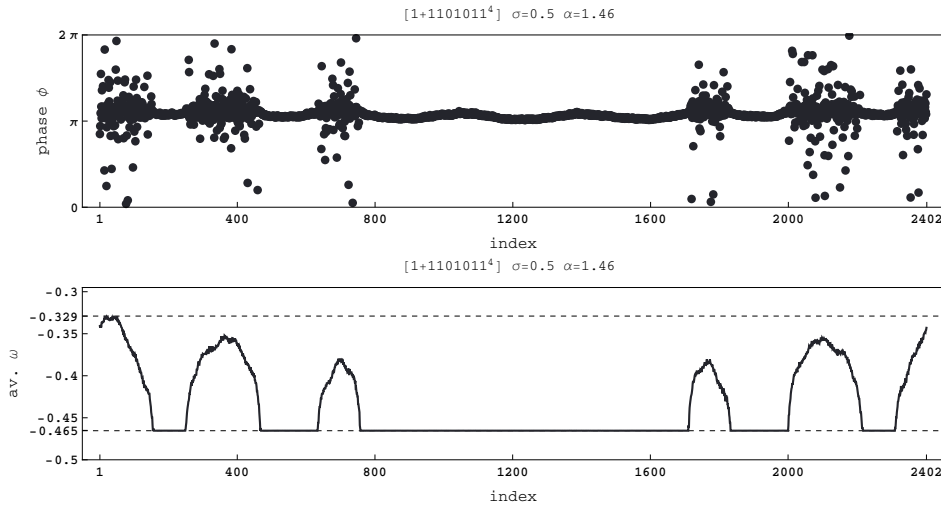


Figure 34 A 5-fold chimera state in a $[1 + 1101011^4]$ -network with $N = 2402$ oscillators. Although the number of connections of each oscillator is the same as in a $[1 + 1110110^4]$ -network (see 32) the average velocities are different in this configuration.

5 Conclusions

The idea of fractally coupled networks in the here presented form gives many ideas for further research. Unfortunately only a small number of networks were researched compared to the number of possible networks. But already in this small number of networks some interesting patterns have been found. The oscillators were able to form chimera states of different structures. Some chimeras were found to exist in different ways but are actually the same. This resulted in a lot of questions about the network. Unfortunately most time was then put into figuring out the complexities of the network structure and in the end having a very obvious solution: It turns out the classical way of thinking about these networks as a ring seems too simple. The simple method of sorting the vertices in a different order already shows that sometimes hidden patterns can be found like a higher coherency of adjacent oscillators (see mid picture in 31). Although it worked, the method of sorting the ring by another increment (7) is probably too simple. In the example used the number of nodes was chosen to be a prime number so no increment could be a divisor of N . In the chimera states where this idea was used the number of nodes was $N = 626$ and none of the increments 5, 25 and 125 were divisors of N . So it was possible to reach every node by this simple sorting. Also only coupling distances that were a power of 5 were checked instead of possibly all coupling distances (some then being a divisor of N). In the future some other methods should be thought of to chose even better suited representations of the networks in order to bring closely coupled oscillators nearer together. The representation of it being a simple ring with a singular form will likely have to be abandoned.

While analysing the data it also turned out that the shaped random initial conditions for the calculations were based on an assumption that turned out to be wrong.

The shape of the random distribution used here has a local coherent neighborhood. In many chimera states coherent oscillator were not necessarily close to each other. So with more time even more chimeras could be found in already studied networks by different initial conditions.

The local order parameter shows to be too simple in the context of mostly non-locally coupled networks. The original idea of it is that local proximity (locality of index) of nodes means a stronger connection of the two. Incidentally this is true for k -nearest neighbor coupling or coupling schemes with decreasing coupling strength for further distances. Due to the relative spatial proximity of strongly coupled oscillators the patterns of coherency and incoherency will be found to be local neighborhoods. Two nodes A and B in close proximity will likely be connected directly and will also be connected to a set of mostly the same nodes $[C_1, C_2, C_3, \dots]$. When the distance of A and B increases, the number of nodes C_i connected to both A and B is decreasing until it is reaching 0. That is a very intuitive relationship of proximity and strength of connection. But with the gap- and fractally coupled networks this relationship is gone. Here there is no general correlation between local proximity and strength of coupled (either directly or via shared connected) nodes anymore that justifies the original assumption for the use of the local order parameter. There may exist many cases of gap- or fractally coupled networks where due to the coupling schemes a local order parameter still seems to be a good tool for finding patterns of coherency (23.) But since patterns of coherency and decoherency are found in oscillators that are stronger connected an order parameter is needed that can identify stronger coupled nodes.

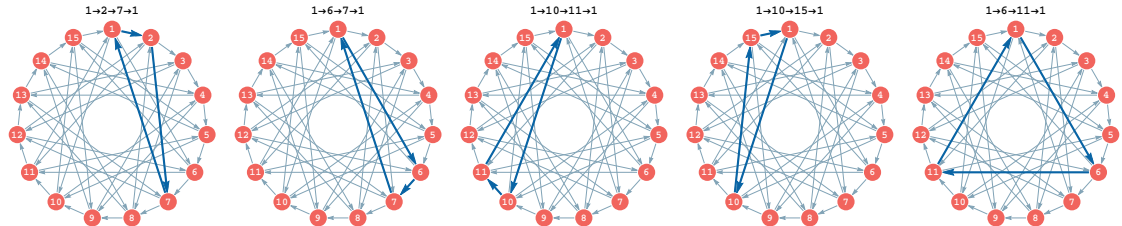


Figure 35 In a directed network of $N = 15$ nodes with edges $i \rightarrow i + k$ with $k \in [1, 5, 9]$ the network has only directed edges resulting in no pairwise coupled nodes (light blue). When looking for triples of nodes (thick dark blue arrows) that start and end with node 1 we find the 5 shown above.

This is especially difficult for directed networks (28). If there is a pair of edges $A \rightarrow B$ and $B \rightarrow A$ the nodes A and B are strongly connected. This pair can also be seen as a small sub-circle that reaches its starting point with only 2 edges ($A \rightarrow B \rightarrow A$). But in directed networks direct pairs may be missing and instead three edges or more are needed to reach the starting point. $A \rightarrow B \rightarrow \dots \rightarrow A$. An order parameter will have to find a measure of coupling strength of nodes before deciding which of them to take into account. In the example (see 35) 5 triples of vertices are identified that all start and end at vertex 1. Among the vertices in all 5 sub-circles some are part of several sub-circles (The nodes [6, 7, 10, 11] each appear

in 2 of the 5 sub-circles). Nodes that appear several times are probably stronger connected to 1. Additionally node 1 will also appear a number of times in sub-circles that start and end at *other* nodes. With increasing non-locality of coupling an order parameter will likely have to take that into account.

6 Possible further research

- More networks should be studied in detail in order to compare them with each other. Possibly finding similarities and categories of networks (symmetrical coupling, asymmetrical coupling, compact bases, ...)
- Different oscillator models should be used in calculations (e.g Kuramoto model with inertia, FitzHugh-Nagumo (FHN), Saddle Node Infinite Period(SNIPER), (leaky) integrate-and-fire and many more.)
- Using non-integer values in the base could likely be interesting e.g. $[1, 0, 1/2] \rightarrow [1, 0, 1/2, 0, 0, 0, 1/2, 0, 1/4]$ (an element c_i is replaced by the base b multiplied with c_i .) For the use of oscillator models with complex coupling values the base b could even consist of complex values.
- a good way of analyzing the coherency of oscillators according to the coupling has yet to be developed. This seems to be especially important for asymmetrical coupling like $b = [11000]$ since a local order parameter can be misleading for almost purely non-local coupling schemes.
- by choosing initial conditions more cleverly additional chimera states could be found.
- due to the exponentially increasing networks and calculation-time it is difficult to study networks of the same base for *many* iterations. This would be an interesting subject as well.

References

- [ABR04] D. M. Abrams and S. H. Strogatz: *Chimera states for coupled oscillators*, Phys. Rev. Lett. **93**, 174102 (2004).
- [HAM07] C. Hammond, H. Bergman, and P. Brown: *Pathological synchronization in Parkinson's disease: networks, models and treatments*, Trends Neurosci. **30**, 357–364 (2007).
- [HIZ13] J. Hizanidis, V. Kanas, A. Bezerianos, and T. Bountis: *Chimera states in networks of nonlocally coupled hindmarsh-rose neuron models*, Int. J. Bifurcation Chaos **24**, 1450030 (2014).
- [LAU2015] J. D. Hon Wai Lau: *Linked and knotted chimera filaments in oscillatory systems*, arXiv:1509.02774 (2015).

- [KUR02a] Y. Kuramoto and D. Battogtokh: *Coexistence of Coherence and Incoherence in Nonlocally Coupled Phase Oscillators.*, Nonlin. Phen. in Complex Sys. **5**, 380–385 (2002).
- [MAI15] Y. Maistrenko, O. Sudakov, O. Osiv, and V. Maistrenko: *Chimera states in three dimensions*, New. Journ. Phys. **17**, 073037 (2015).
- [OME10a] O. E. Omel’chenko, M. Wolfrum, and Y. Maistrenko: *Chimera states as chaotic spatiotemporal patterns*, Phys. Rev. E **81**, 065201(R) (2010).
- [OME11] I. Omelchenko, Y. Maistrenko, P. Hövel, and E. Schöll: *Loss of coherence in dynamical networks: spatial chaos and chimera states*, Phys. Rev. Lett. **106**, 234102 (2011).
- [OME12] I. Omelchenko, B. Riemenschneider, P. Hövel, Y. Maistrenko, and E. Schöll: *Transition from spatial coherence to incoherence in coupled chaotic systems*, Phys. Rev. E **85**, 026212 (2012).
- [OME13] I. Omelchenko, O. E. Omel’chenko, P. Hövel, and E. Schöll: *When non-local coupling between oscillators becomes stronger: patched synchrony or multichimera states*, Phys. Rev. Lett. **110**, 224101 (2013).
- [OME15] I. Omelchenko, A. Provata, J. Hizanidis, E. Schöll, and P. Hövel: *Robustness of chimera states for coupled FitzHugh-Nagumo oscillators*, Phys. Rev. E **91**, 022917 (2015).
- [OME15a] I. Omelchenko, A. Zakharova, P. Hövel, J. Siebert, and E. Schöll: *Non-linearity of local dynamics promotes multi-chimeras*, Chaos **25**, 083104 (2015).
- [ROD15] F. A. Rodrigues, T. K. D. Peron, P. Ji, and J. Kurths: *The Kuramoto model in complex networks*, Phys. Rep. (2015).

7 Appendix

Some additional graphs of chimera states. Some of them also by different indices (indicated within the plot.).

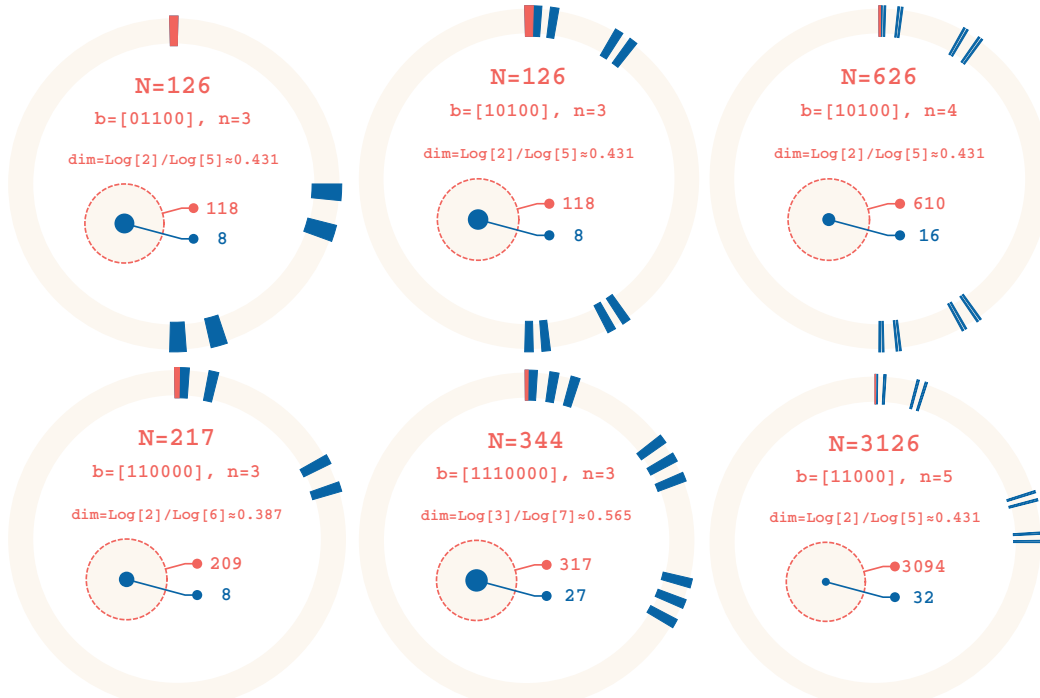


Figure 36 Some visualizations of the networks in the appendix.

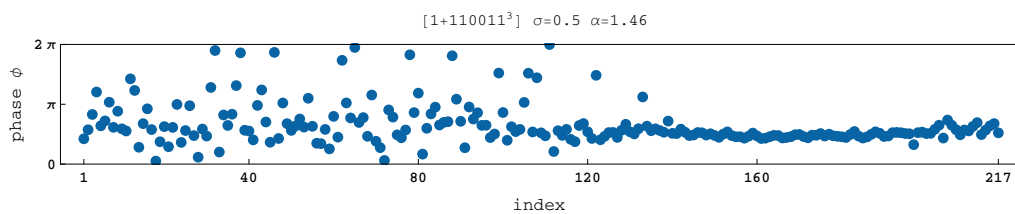


Figure 37 A simple single chimera in a smaller $[1 + 110011^3]$ -network.

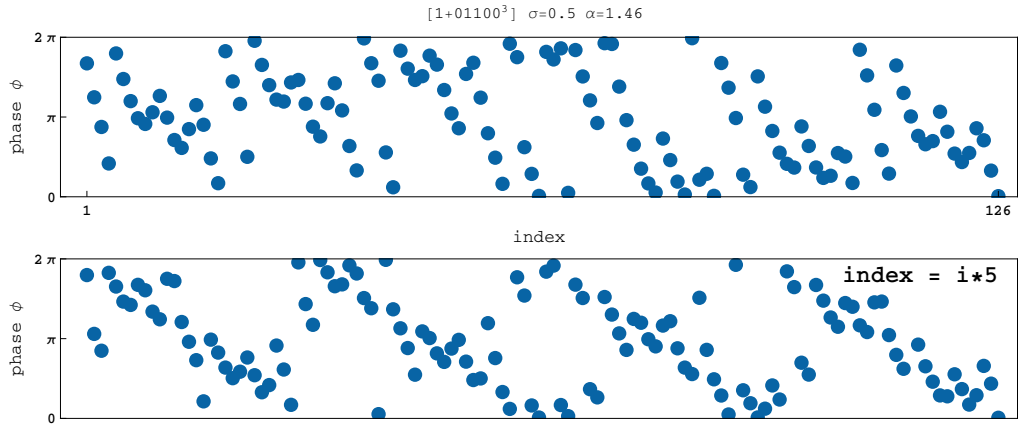


Figure 38 A chimera in a $[1 + 01100^3]$ -network. Normal index (top) and i_5 underneath.

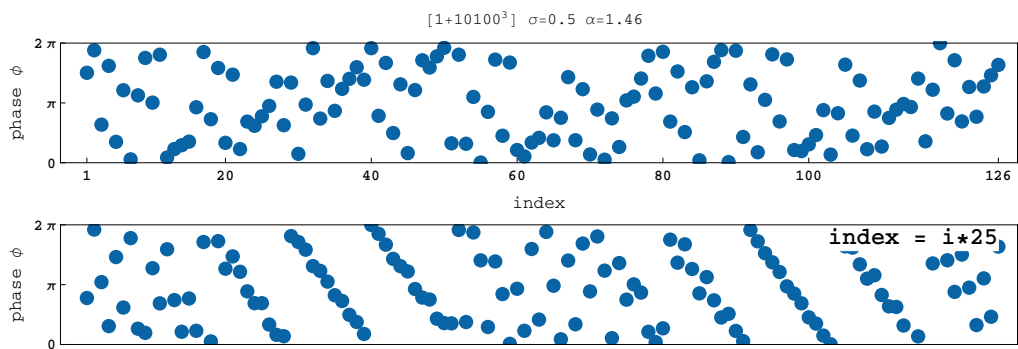


Figure 39 A chimera in a $[1 + 10100^3]$ -network. Normal index (top) and i_{25} underneath.

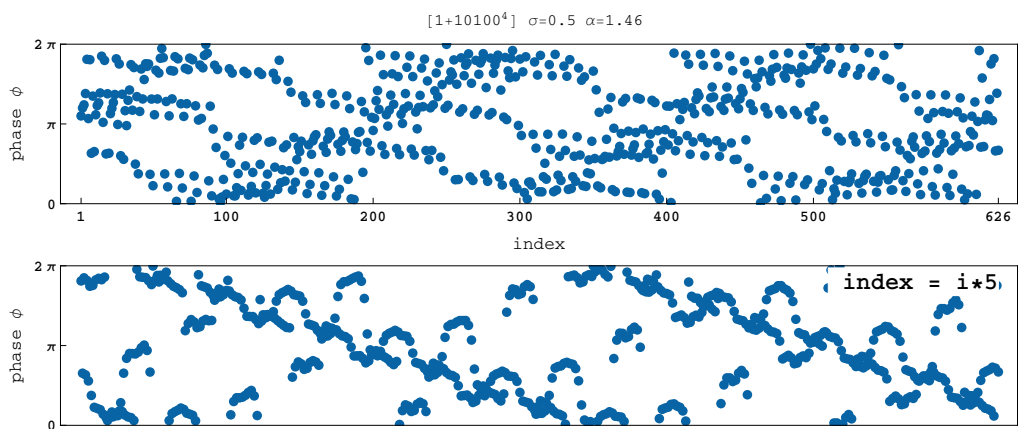


Figure 40 A chimera in a $[1 + 10100^4]$ -network. Normal index (top) and i_5 underneath.

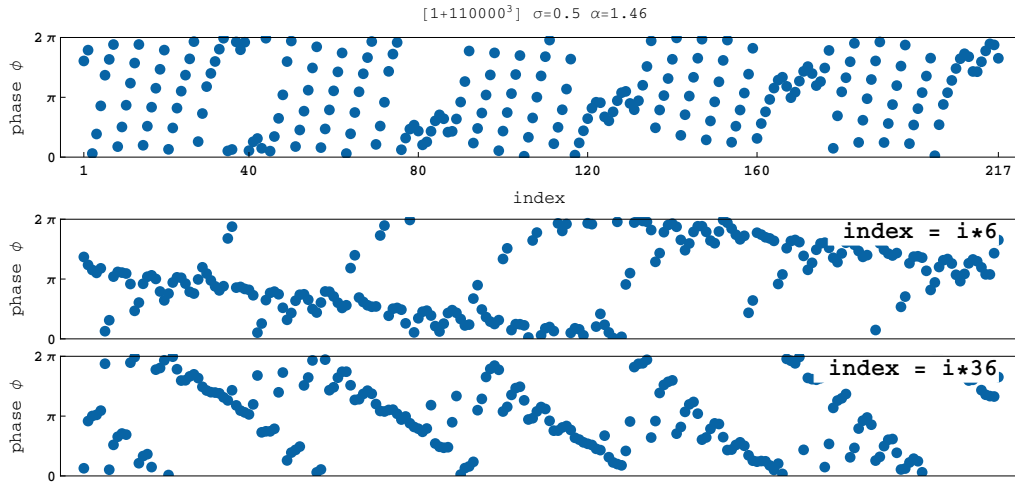


Figure 41 A chimera in a $[1 + 110000^3]$ -network. Normal index (top), i_6 , and i_{36} underneath.

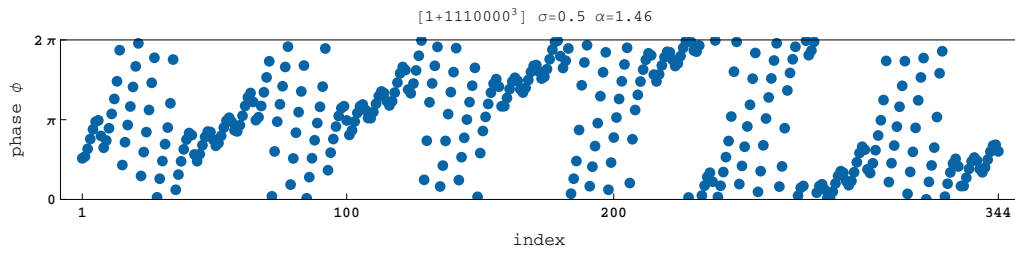


Figure 42 A chimera in a $[1 + 1110000^3]$ -network.

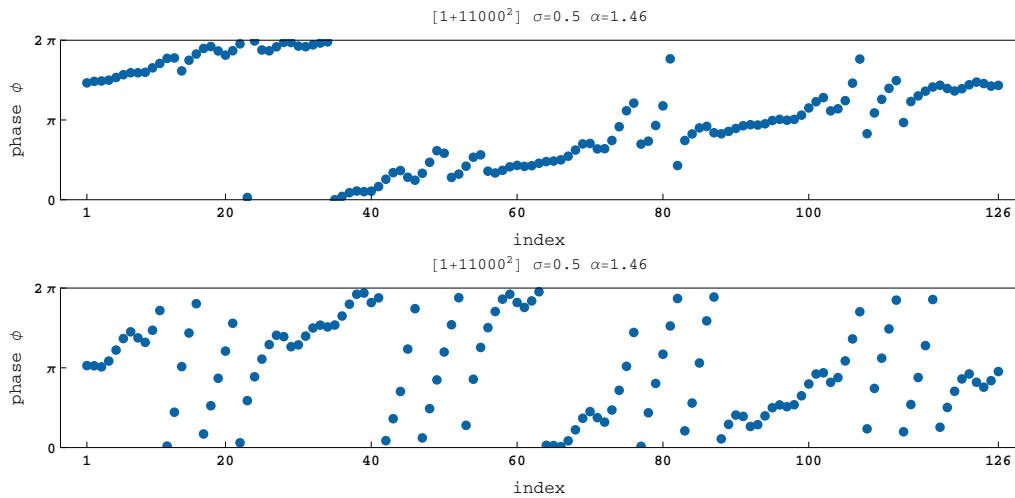


Figure 43 Two chimera in a $[1 + 11000^2]$ -network. At least one of them has similarities with the chimera state A (28).

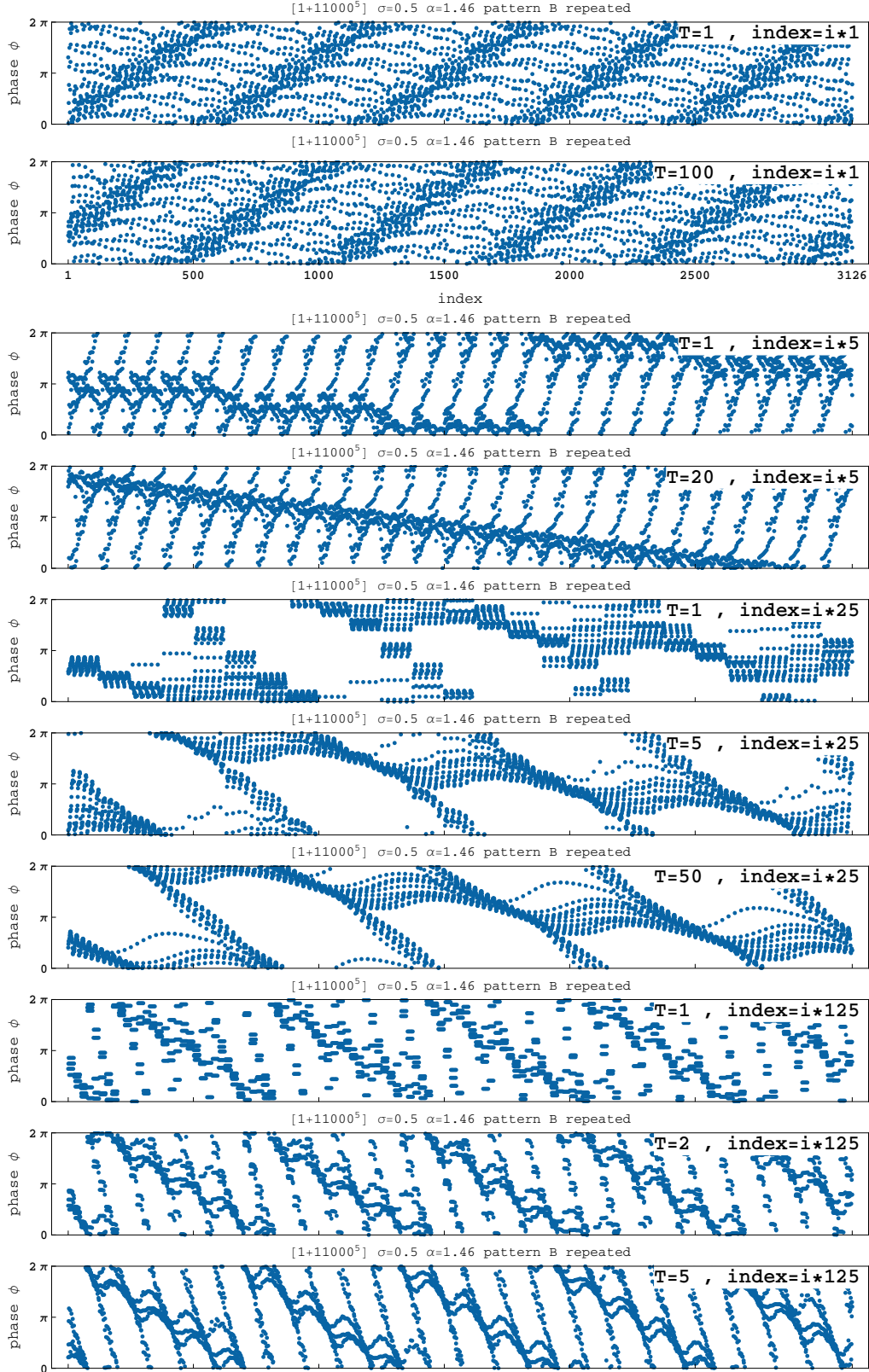


Figure 44 This pattern did not naturally emerge but was created artificially: When simply repeating the chimera B (28) and using it in $[1+11000^5]$ the network is quickly 'smoothing' out the edges. Although this is not visible in the original ordering (2 topmost plots) it can be seen when changing the index all beneath). The new chimera state was stable. This also worked for chimera A (not shown).

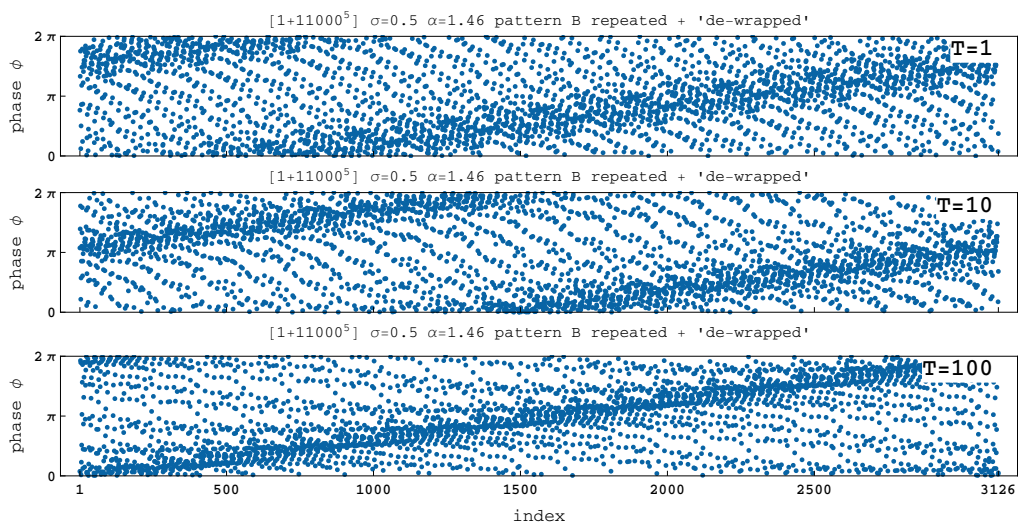


Figure 45 Here the chimera state B of the network $1 + [11000^4]$ was not only repeated 5 times to reach $N = 1 + 5^5 = 3126$ oscillators. Because of the repetition a phase shift (or 'wrap-around') is also multiplied 5 times (see 44). This was corrected by subtracting a phase shift of $(5 - 1)2\pi i/N$. The calculation is shown for the $T = 1, 10, 100$ of the calculation. After an initial transition the pattern remains stable. This process (repeating the pattern and changing the number of 'wrap-arounds' back to 1 did only work for chimera B and not for A .)